

## Supplementary Information Appendix

**Title:** Mechanistic evidence for tracking the seasonality of photosynthesis with solar-induced fluorescence

**Journal:** *Proceedings of the National Academy of Sciences*

**Authors:** Troy S. Magney<sup>1,2</sup>, David R. Bowling<sup>3</sup>, Barry A. Logan<sup>4</sup>, Katja Grossmann<sup>5</sup>, Jochen Stutz<sup>5</sup>, Peter D. Blanken<sup>6</sup>, Sean P. Burns<sup>6,7</sup>, Rui Cheng<sup>1</sup>, Maria A. Garcia<sup>3</sup>, Philipp Köhler<sup>1</sup>, Sophia Lopez<sup>4</sup>, Nicholas Parazoo<sup>2</sup>, Brett Raczka<sup>3</sup>, David Schimel<sup>2</sup>, Christian Frankenberg<sup>1,2</sup>

**Affiliations:**

<sup>1</sup>California Institute of Technology, Division of Geological and Planetary Sciences, Pasadena, CA

<sup>2</sup>Jet Propulsion Laboratory, California Institute of Technology, Carbon Cycle and Ecosystems, Pasadena, CA

<sup>3</sup>University of Utah, School of Biological Sciences, Salt Lake City, UT

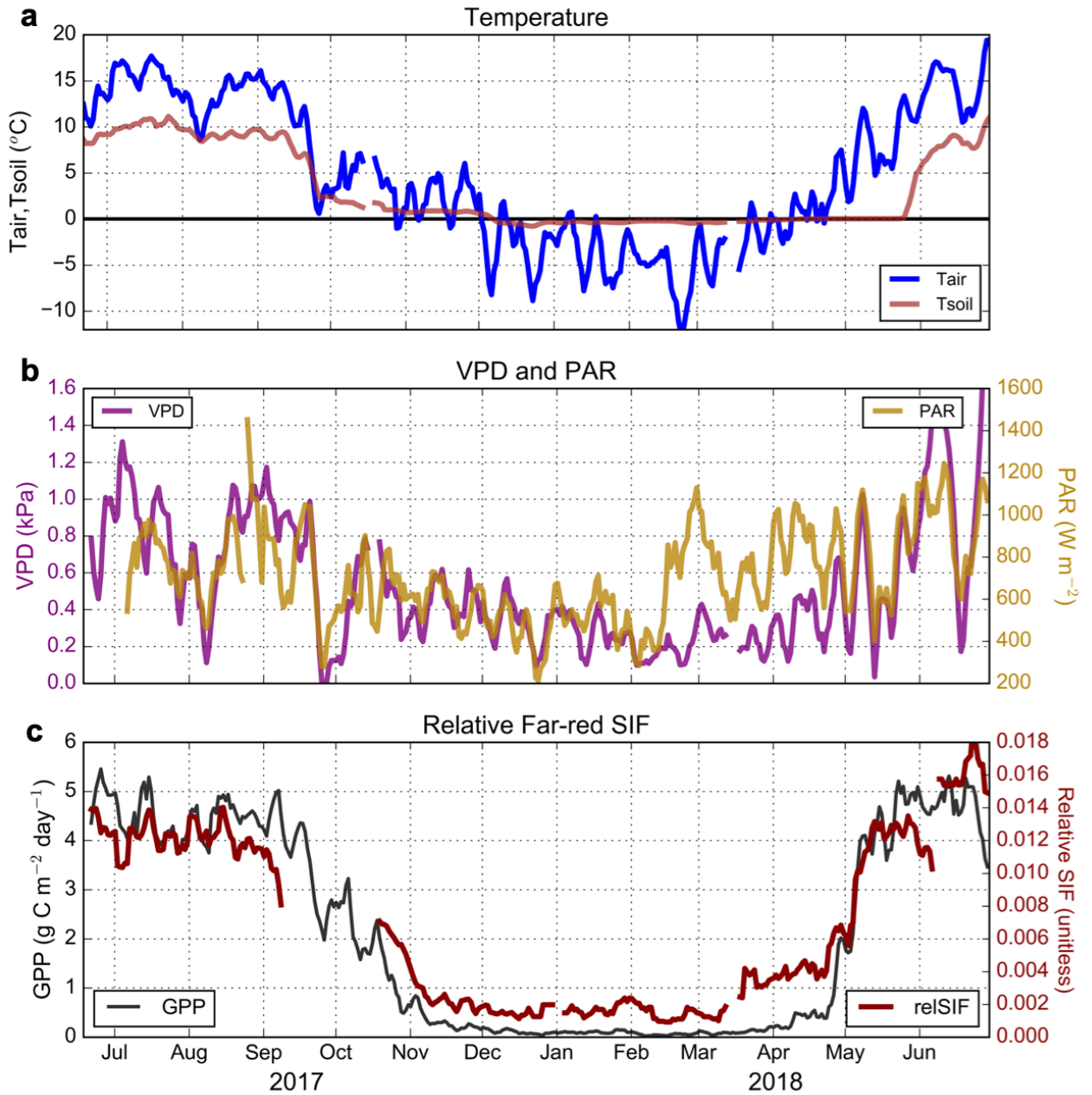
<sup>4</sup>Bowdoin College, Department of Biology, Brunswick, ME

<sup>5</sup>University of California Los Angeles, Department of Atmospheric and Oceanic Sciences, Los Angeles, CA

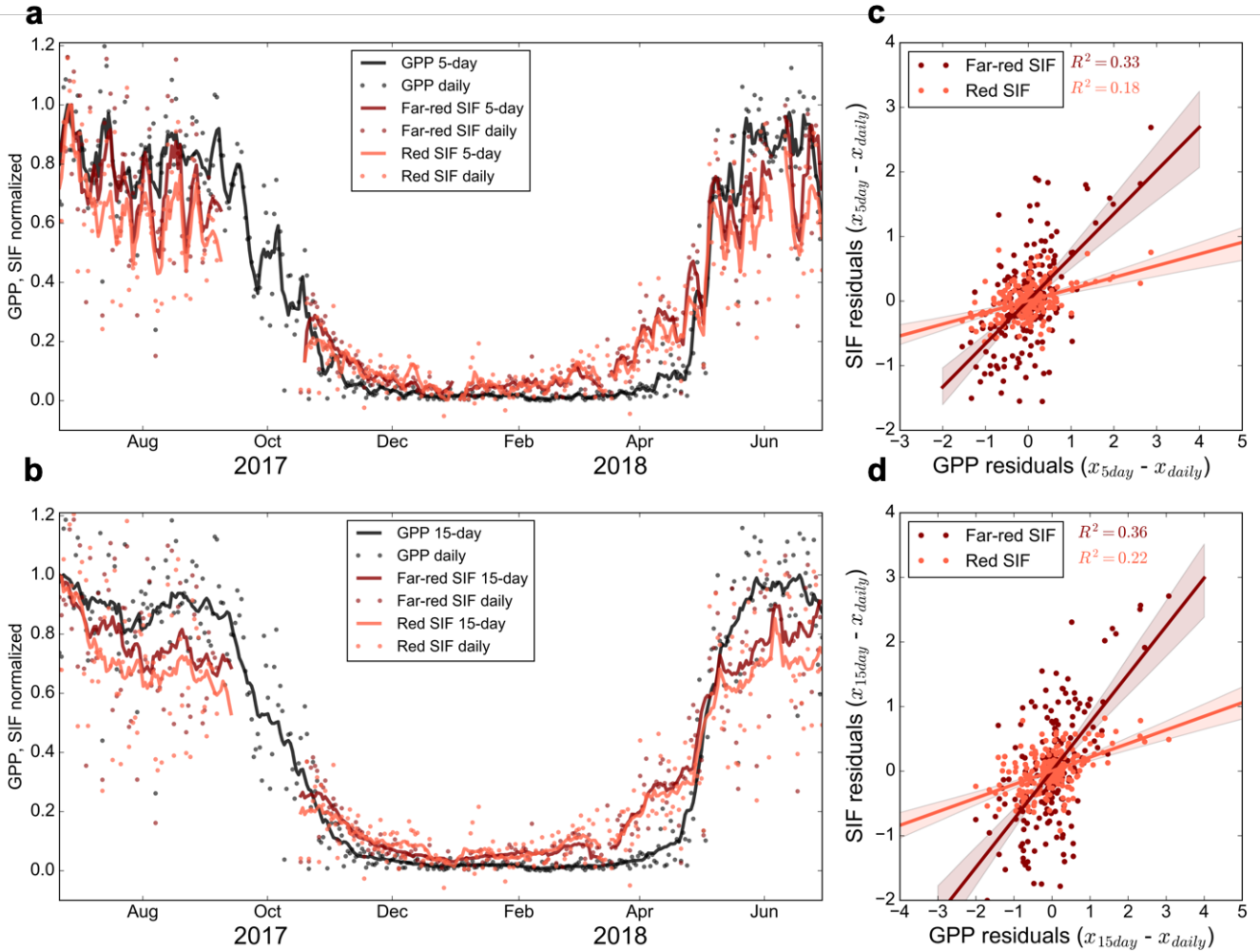
<sup>6</sup>University of Colorado, Boulder, Department of Geography, Boulder, CO

<sup>7</sup>National Center for Atmospheric Research, Boulder, CO

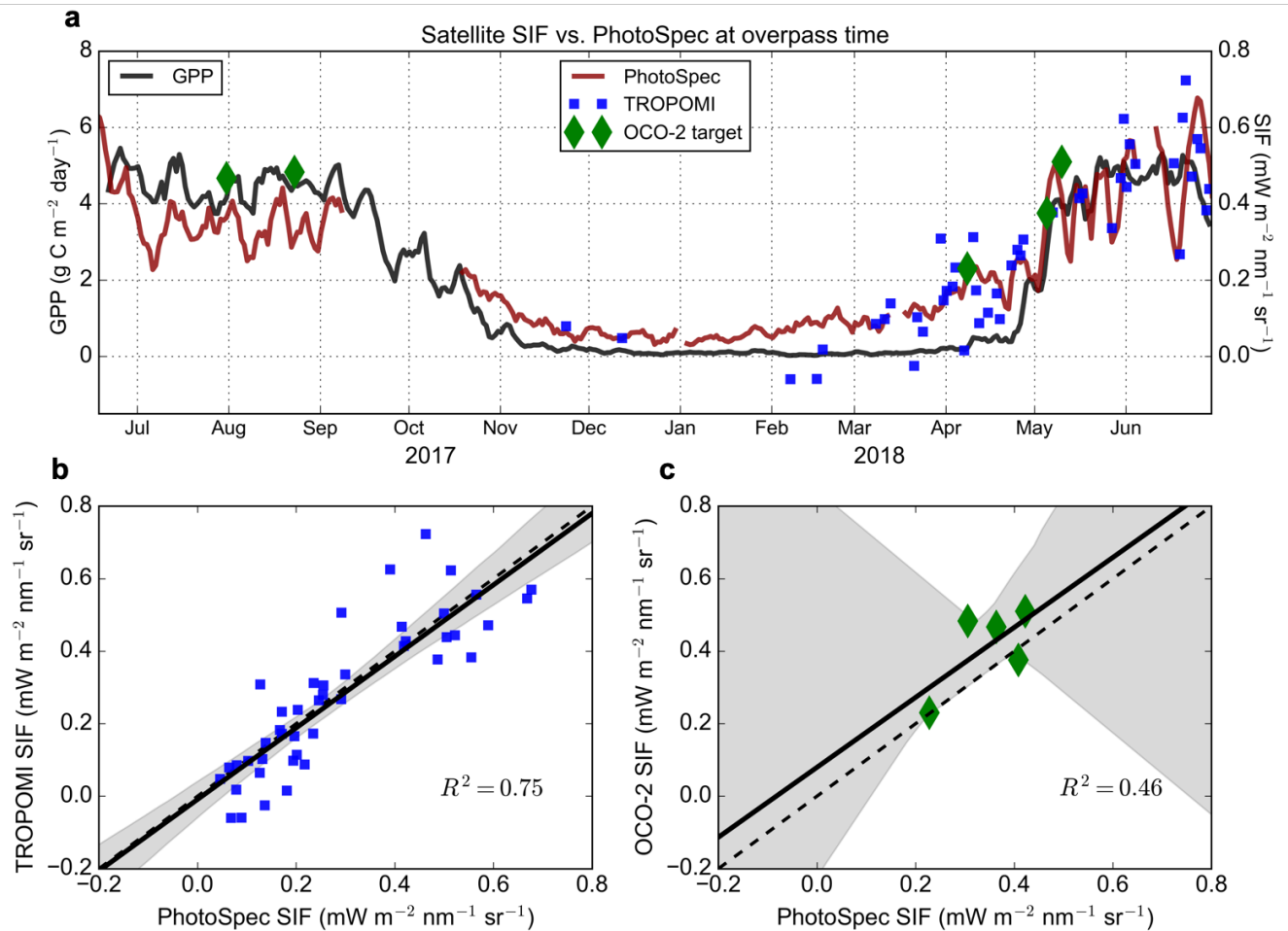
Supplementary figures:



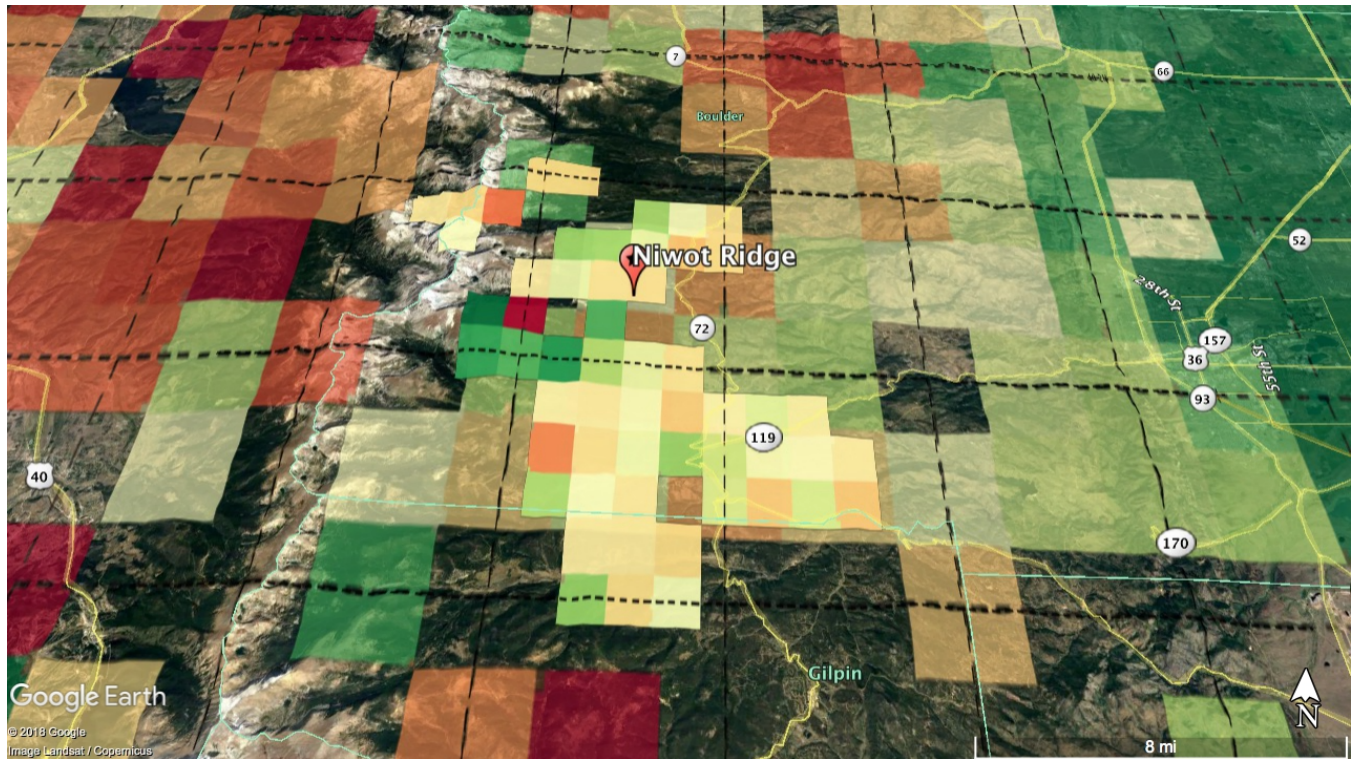
**Supplementary Fig. S1:** Five-day running means of GPP against (a) air and soil temperature; (b) Vapor pressure deficit (VPD) and photosynthetically active radiation (PAR); (c) relative SIF. Relative SIF was computed at Far-red SIF / reflected radiance in the retrieval window (NIR).



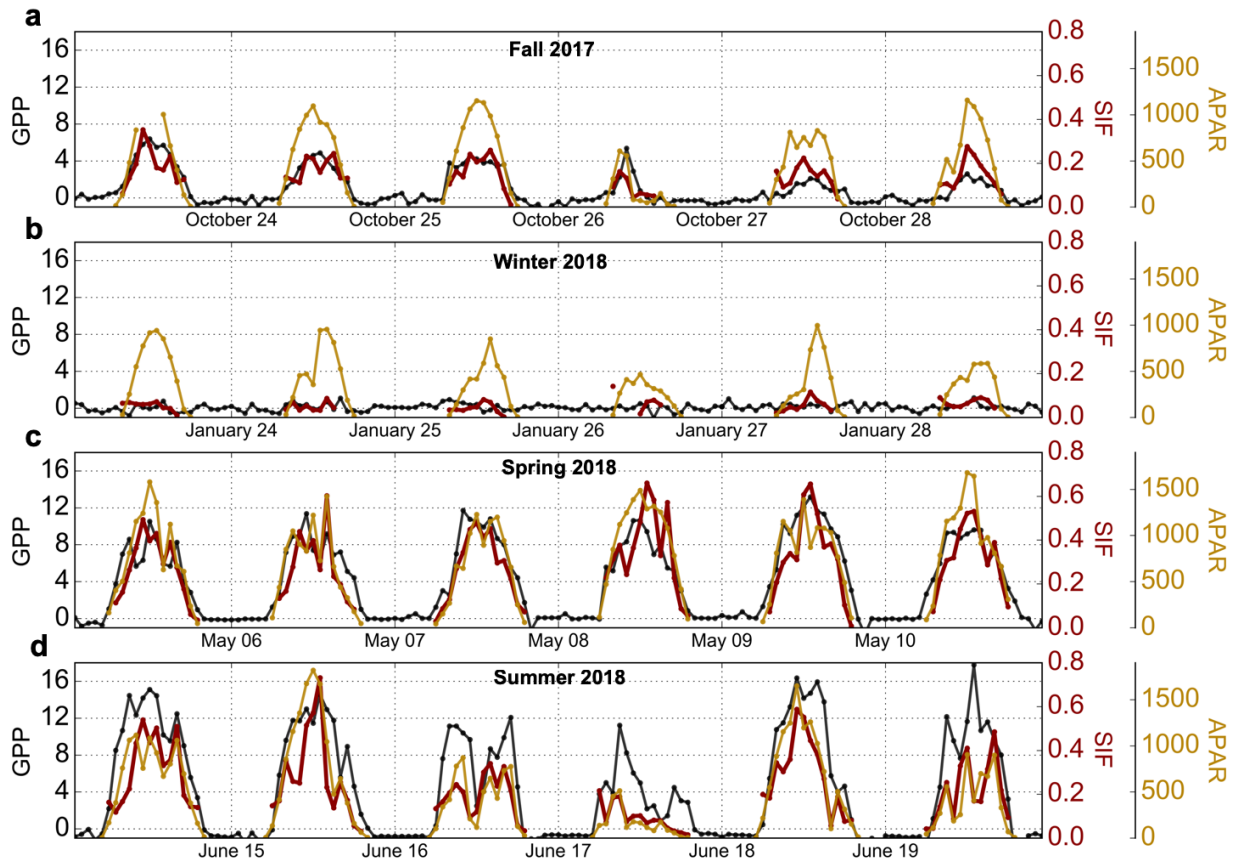
**Supplementary Fig. S2:** GPP and SIF normalized by the seasonal maximum of each to observe day-to-day dynamics, largely driven by variability in PAR. The daily data are represented by dots. (a) 5-day running mean as shown in Fig. 1. (b) Same as above except with a 15 day-running mean. (c) SIF residuals against GPP residuals from the 5-day running mean of each. Both relationships are statistically significant ( $p < 0.05$ ). (d) SIF residuals against GPP residuals from the 15-day running mean. All relationships are statistically significant ( $p < 0.05$ ). Shaded regions represent one standard error.



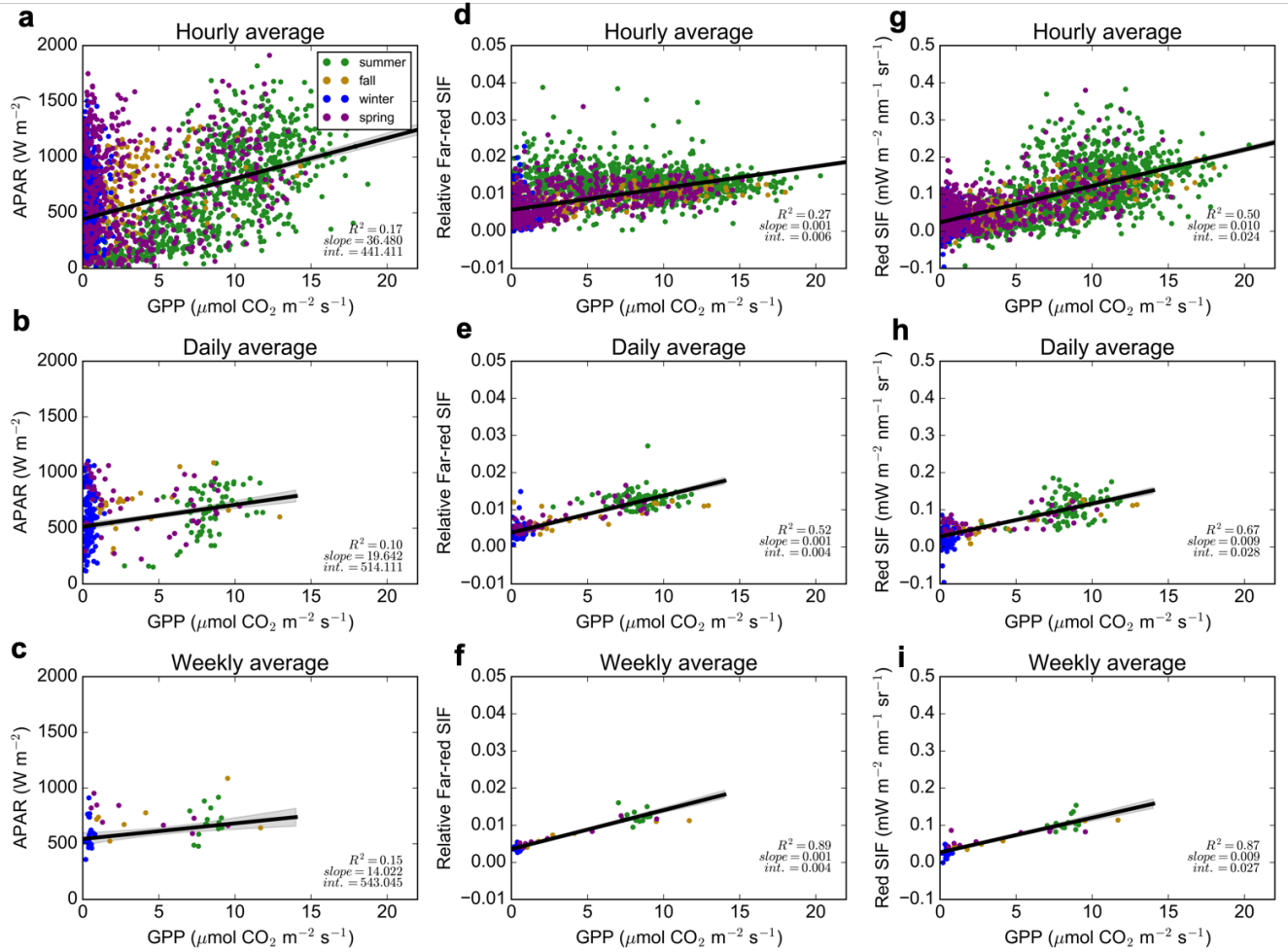
**Supplementary Fig. S3:** (a) Seasonal correspondence between tower far-red SIF, TROPOMI, and OCO-2 SIF. TROPOMI data were only available beginning November 2017, and all data are shown (no cloud filter applied). (b) The correlation between TROPOMI SIF and PhotoSpec SIF was statistically significant ( $p < 0.05$ ), and 1:1 line indicated by dashed line. (c) Correlation between OCO-2 ‘target’ mode and tower SIF. Error bars indicate a 95% confidence interval around the line of best fit. Slightly negative SIF values can occur due to the retrieval uncertainty, particularly in winter when the SIF signal is small (Köhler et al., 2018). TROPOMI and OCO-2 data are from the native resolution, not the gridded product shown in Fig. S4.



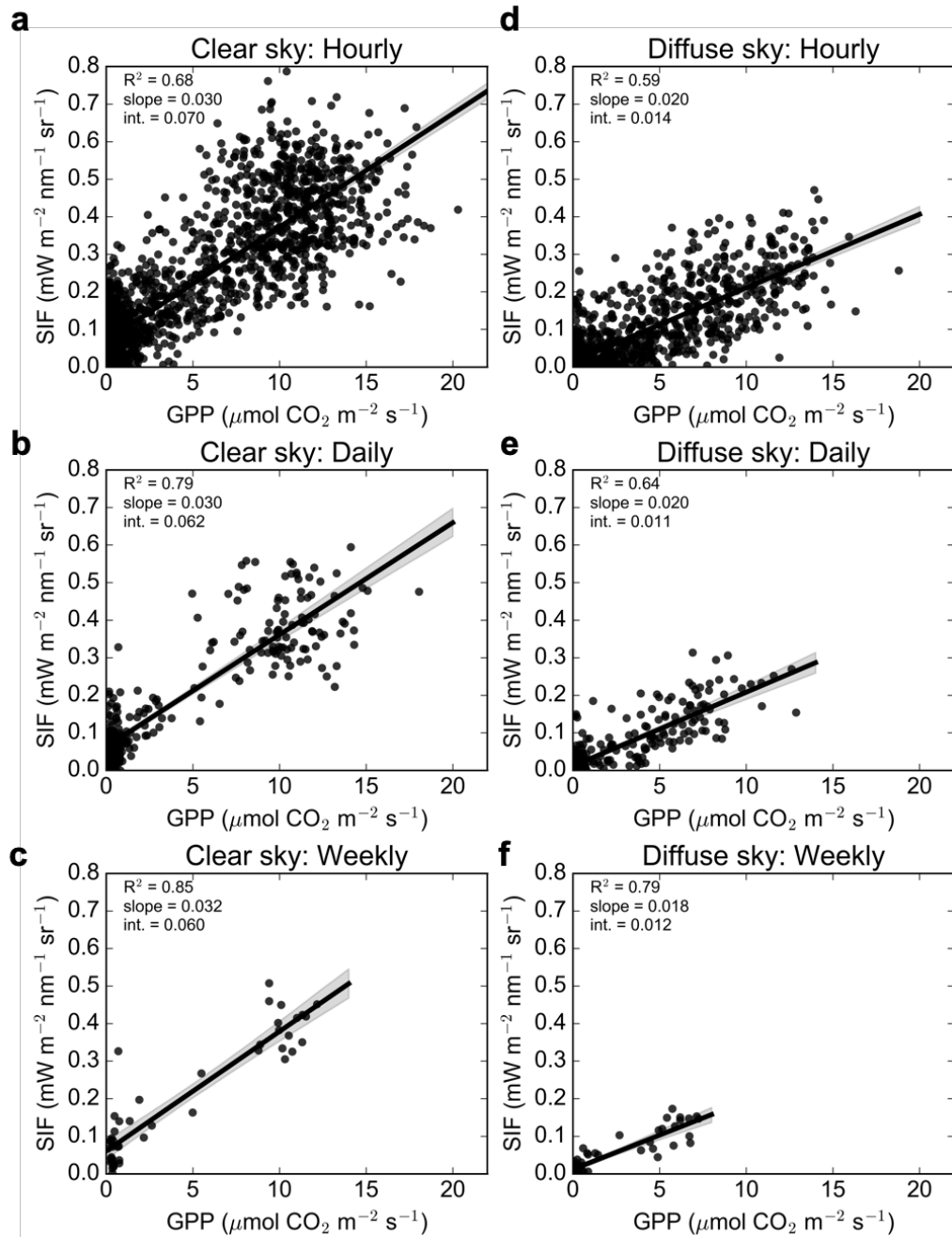
**Supplementary Fig. S4:** Map of gridded TROPOMI and OCO-2 SIF data overlaid on a Google Earth image to highlight topography and region of satellite coverage. The transparent pixels represent TROPOMI SIF data (gridded to  $0.05 \times 0.05$  degrees), and the solid pixels represent OCO-2 target mode data (gridded to  $0.02 \times 0.02$  degrees). Note that these pixel sizes are reasonably larger than the actual footprint size of the data used in Fig. S3. Data are presented in this fashion as this is typically the resolution these data products are provided to the community in. The colors represent the average SIF value during the entire year of 2018, with the green values representing higher values and the red representing lower values.



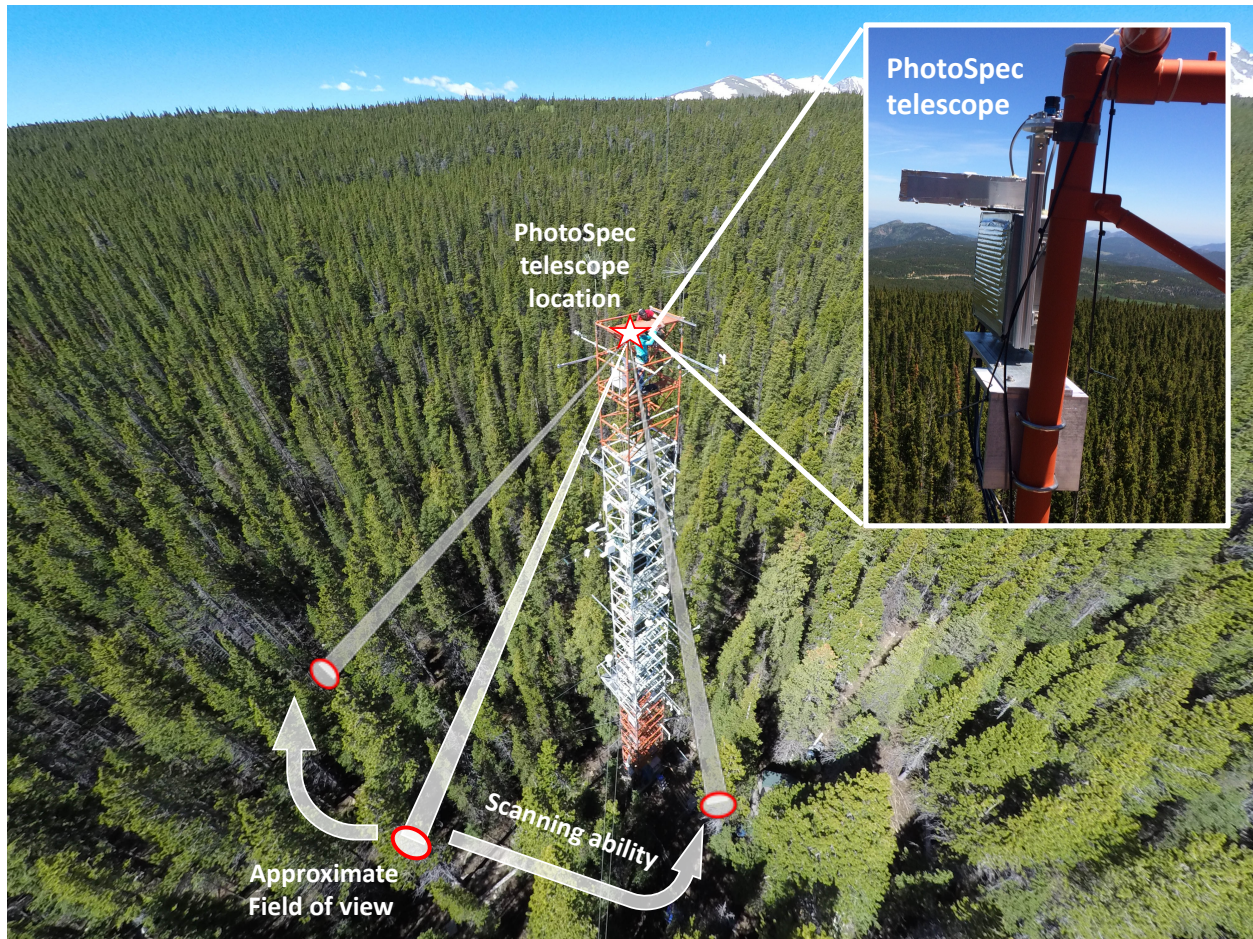
**Supplementary Fig. S5.** Hourly averages of Gross Primary Production (GPP  $\mu\text{mol m}^{-2} \text{s}^{-1}$ , black), Far-red solar-induced fluorescence (SIF,  $\text{mW m}^{-2} \text{nm}^{-1} \text{sr}^{-1}$ , dark-red) and Absorbed Photosynthetically Active Radiation (APAR,  $\text{W m}^{-2}$ , gold) of the canopy. (a) October 23 – October 28, 2017; (b) January 23– January 28, 2018; (c) May 5 – May 11, 2018; (d) June 14 – June 19, 2018.



**Supplementary Fig. S6:** (a-c) Relationships between APAR and GPP at hourly, daily and weekly timescales. (d-f) Relationships between relative far-red SIF and GPP at hourly, daily, and weekly timescales. (g-i) Relationships between red SIF and GPP at hourly, daily, and weekly timescales. All reported results were statistically significant at  $p < 0.05$ .



**Supplementary Fig. S7:** Relationship between SIF and GPP under clear (a-c) and diffuse (d-f) sky conditions, at hourly (a,d), daily (b,e), and weekly (c,f) time intervals. Shaded regions represent one standard error of the mean, and all reported relationships are statistically significant at  $p < 0.05$ . Clear sky was defined as top-of-canopy shortwave radiation/top-of-atmosphere shortwave radiation  $> 0.5$ .



**Supplementary Fig. S8:** A photo of the Niwot Ridge Tower taken from a drone, with the approximate instrument field of view indicated by red circles. The star indicates the tower location on the top of tower, with a zoom in of the instrument itself in the top right. The arrows are to demonstrate the scanning ability of PhotoSpec.

<b>SIF v APAR</b>	<b>Slope</b>	<b>Intercept</b>	<b>R<sup>2</sup></b>
Summer	0.00035	0.032	0.70*
Fall	0.00018	-0.009	0.37*
Winter	0.00008	-0.006	0.30*
Spring	0.00022	0.003	0.47*
<b>SIF v GPP</b>	<b>Slope</b>	<b>Intercept</b>	<b>R<sup>2</sup></b>
Summer	0.029	0.0239	0.45*
Fall	0.022	0.051	0.50*
Winter	0.045	0.001	0.00
Spring	0.024	0.064	0.47*

**Supplementary Table S1:** Linear regression results for hourly data, broken down by season. Asterisk indicates a significant relationship where  $p < 0.05$ . These data are from the same seasonal periods as Fig. 2.